Temporal Characteristics of Oxygenation-Sensitive MRI Responses to Visual Activation in Humans

Peter Fransson, Gunnar Krüger, Klaus-Dietmar Merboldt, Jens Frahm

Series of single-shot blipped echo-planar images with spin-density weighting and T_2* sensitivity (2.0 T, TR = 400 ms, TE = 54 ms, flip angle = 30°) were used to study the temporal response profiles to repetitive visual activation (5 Hz, reversing black and white checkerboard versus darkness) for protocols comprising multiple cycles of a 1.6-s stimulus in conjunction with a 8.4-s or 90-s recovery phase and a 10-s stimulus with a 20-s or 90-s recovery phase. Analysis of the real-time data from all activated pixels resulted in a strong positive MRI response (mean values 3–6%) as well as a marked poststimulus undershoot (mean values 1–2%, duration 60–90 s) for all paradigms. Repetitive protocols with insufficient recovery periods of 8.4 s or 20 s gave rise to a wraparound effect when analyzing time-locked averages from multiple activation cycles. This problem may lead to an early signal decrease that originates from the ongoing undershoot of preceding activations folded back into the initial latency phase of a subsequent activation. When ensuring complete decoupling of responses to successive stimuli by using a 90-s recovery period, the wraparound effect vanished and an initial dip was observed in one of seven subjects for a 10-s/90-s protocol.

Key words: neuroimaging — human brain; functional activation; brain function; cerebral blood oxygenation.

INTRODUCTION

Functional activation of the human brain may be investigated with use of gradient-echo MRI signals that are sensitized to differences in the intravascular concentration of paramagnetic deoxyhemoglobin (1–5). During task performance, the MRI-detectable changes in cerebral blood oxygenation represent a physiological response coupled with a change in neuronal activity. Continuous monitoring allows mapping of brain functions at high spatiotemporal resolution.

Although early methodological developments have paid little attention to the underlying interplay of hemodynamic and metabolic adjustments, such knowledge is of utmost importance because any alteration of an oxygenation-dependent MR parameter emerges as the result of a complex change in brain physiology. Apart from the desired task-related adaptation in neuronal activity, contributions may arise from other cognitive or emotional processes (e.g., attention and anxiety) or even systemic adjustments (e.g., heart rate and blood pressure). In addition, amplitude and temporal characteristics may be subjected to changes in neurovascular responsiveness in relation to age (e.g., in early infancy and in the elder population), nutrition and medication (e.g., vasoactive and psychotropic drugs), or neuropathology (e.g., cerebrovascular disease). Although pertinent sensitivities of oxygenation-sensitive MR techniques may lead to new clinical applications, they complicate the optimum design of brain-mapping protocols by masking or emphasizing stimulus-related MRI signal changes.

More recent interest in the understanding of functional responses has focused on the temporal evolution of blood oxygenation level dependent (BOLD) contrast during both the early and late phases of brain activation. For example, visual activation over several minutes has led to controversies with regard to the persistence of the MRI signal *increase* that were partially reconciled by the observation of a stimulus dependence of the sustained oxygenation-sensitive response (6–8). On the other hand, an initial fast response yielding an MRI signal *decrease* peaking approximately 2 s after stimulus onset was reported using echo-planar imaging (EPI) at high temporal resolution (9–13), whereas potentially related effects were seen at 0.5 s after stimulus onset using MR spectroscopy (14, 15). These findings resemble data from optical imaging of exposed visual cortex in animals in which intrinsic signals in the red and near-infrared part of the optical spectrum reflect absorption from oxyhemoglobin and deoxyhemoglobin and cytochrome oxidase as well as light scattering (16–18). Deconvolution of the deoxyhemoglobin response suggests an early deoxygenation that may be understood as an immediate increase in oxygen consumption at the site of neuronal activation. Thus, if a corresponding MRI signal decrease or "dip" due to initially elevated deoxyhemoglobin could be reliably detected, it might become a potent marker for very focal changes of neuronal activity. However, it is not entirely clear whether, or to which degree, optical data from animals may be extrapolated for MRI studies of humans. Apart from our limited knowledge about the interplay of activation-induced adjustments of blood flow, blood volume, and oxidative metabolism in humans, both methodologies focus on different tissue elements: whereas MRI detects intravoxel susceptibility changes from all vascular components that contribute to one image voxel, optical experiments commonly exclude all signals from vessels within the used cranial window that are identifiable by visual inspection.

In general, the temporal evolution of functional MRI contrast based on changes in blood oxygenation will be the result of multiple regulative processes with different time constants. Such contributions may critically affect

MRM 39:912–919 (1998)

From Biomedizinische NMR Forschungs GmbH am Max-Planck-Institut für biophysikalische Chemie, Göttingen, Germany.

Address correspondence to: Jens Frahm, Ph.D., Biomedizinische NMR Forschungs GmbH am Max-Planck-Institut für biophysikalische Chemie, D-37070 Göttingen, Germany.

Received September 22, 1997 revised November 11, 1997; accepted November 29, 1997.

P.F. is on leave from the MR Research Center, Karolinska Institutet, Stockholm, Sweden.

0740-3194/98 $3.00

the interpretation of MRI responses, particularly when these are acquired with use of repetitive stimuli. In fact, previous investigations of the early response have used various protocols with stimulus durations ranging from 1.6 to 10 s and control periods of 8.4 to 40 s.

The aim of this study was to specifically address the influence of the paradigm timing on the temporal characteristics of human brain responses to visual activation with special emphasis on the early phase. In all cases, MRI studies were confined to "pure" BOLD contrast, i.e. T_2* sensitivity in the absence of any T_1 weighting, to assess true changes in cerebral blood oxygenation.

METHODS

Subjects and Functional Neuroimaging

A total of 14 healthy volunteers (age range 23–45 years, mean 27 years) underwent MRI examinations at 2.0 T (Siemens Vision, Erlangen, Germany) using the standard imaging head coil. Dynamic oxygenation-sensitized images were obtained using single-shot, blipped gradient-echo EPI (TR = 400 ms, TE = 54 ms, flip angle = 30°) with symmetrical coverage of *k*-space. Functional responses were acquired in a single oblique section along the calcarine fissure at 128 × 128 matrix resolution (FOV = 384 × 384 mm, section thickness = 4 mm) yielding an echo train length of 102 ms for a receiver bandwidth of 188 kHz.

Visual stimulation was accomplished by a projection setup covering 40° × 30° of the subject's visual field (Schäfter & Kirchhoff, Hamburg, Germany). The stimulus consisted of a checkerboard pattern representing a radial arrangement of 16 wedges formed by seven to eight black and white segments at equal radial distance. All black and white segments reversed color 10 times per second, i.e., repetition of a full cycle of black and white color was at a frequency of 5 Hz. A central red cross was used as a fixation point. The control state was darkness without a fixation cross in all studies. Subjects were instructed to keep their eyes open and maintain constant attention throughout the experiments.

Activation Protocols

This study compared four different stimulation paradigms with identical stimuli but different timings. All protocols contained an initial baseline period of 60 s to allow for the establishment and determination of prestimulation control values for the BOLD MRI signal strength. This phase was followed by repetitive cycles of alternating periods of stimulation (reversing checkerboard) and recovery (darkness) with timings described below. A final recovery phase of 100-s duration was added to the end of all paradigms to ensure return to prestimulation conditions. In general, data from the first 8 s of each protocol (20 images) were discarded to account for equilibration purposes.

The first protocol closely replicated the visual paradigm design of ref. 11, i.e., a stimulus duration of 1.6 s followed by 8.4 s of control in a loop of 12 cycles. The second protocol kept the stimulus duration of 1.6 s but prolonged the control period to 90 s. The number of cycles was set to four to keep the total duration of the experiment less than 10 min. The third protocol used a 10-s stimulus in combination with a 20-s control phase comparable to a design used in ref. 10. This cycle was repeated sixfold. Again, the fourth protocol kept the 10-s stimulus duration of the third protocol while extending the control period to 90 s in a loop of four cycles.

Data Analysis

Activated pixels were identified by a cross-correlation analysis (19) of individual pixel intensity time courses with a reference function representing the stimulus protocol with inclusion of an early signal decrease after stimulus onset. The actual reference function was a rectangular waveform with amplitudes of −1 for the initial dip (0.4–4.0 s after stimulus onset), 0 for baseline and control periods, and 1 for stimulation phases (shifted by 4.0 s with respect to stimulus onset). MRI signal intensities were normalized to prestimulation baseline, i.e., the mean MRI signal intensity before the first stimulation period, before averaging across subjects. Quantitative maps of correlation coefficients were obtained by cross-correlation with the reference function and a statistical analysis that, based on the individual noise distribution, uses a high threshold for identifying activated centers ($P \leq 0.0001$) and integration of neighboring pixels for area delineation (20). Normalized signal intensity time courses from dynamic oxygenation-sensitized EPI were obtained from all activated pixels admitted by the analysis. Unless otherwise stated, they represent mean curves averaged across subjects.

RESULTS AND DISCUSSION

The contrast-to-noise ratio and spatial resolution of an oxygenation-sensitized echo-planar image, as used here for mapping BOLD MRI signals that are based on pure T_2* weighting, are shown in Fig. 1A. In general, activation maps for individual subjects revealed a spatial congruence of activated areas for all protocols. This is demonstrated in Figs. 1B through 1D for one subject and three protocols. When averaged across subjects, the mean numbers of activated pixels (area) were 128 pixels (1150 mm^2) for the 1.6-s/8.4-s protocol, 99 pixels (893 mm^2) for the 1.6-s/90-s protocol, 199 pixels (1792 mm^2) for the 10-s/20-s protocol, and 174 pixels (1563 mm^2) for the 10-s/90-s protocol. Factors that might be responsible for these differences comprise both physiological reasons such as stimulus duration and aspects of statistical analysis, e.g., thresholding in relation to preset limits and actual contrast-to-noise ratio.

The 1.6-s/8.4-s Protocol

In Fig. 2, the mean signal intensity time course for the 1.6-s/8.4-s visual activation protocol is shown in real time (Fig. 2A) as well as in the form of time-locked averages of either all 12 (Fig. 2B) or only the first four activation cycles (Fig. 2C), as in ref. 11. The qualitative response behavior elicited by this protocol is identical to what is commonly reported for studies involving repetitive visual activation. For example, the apparent de-

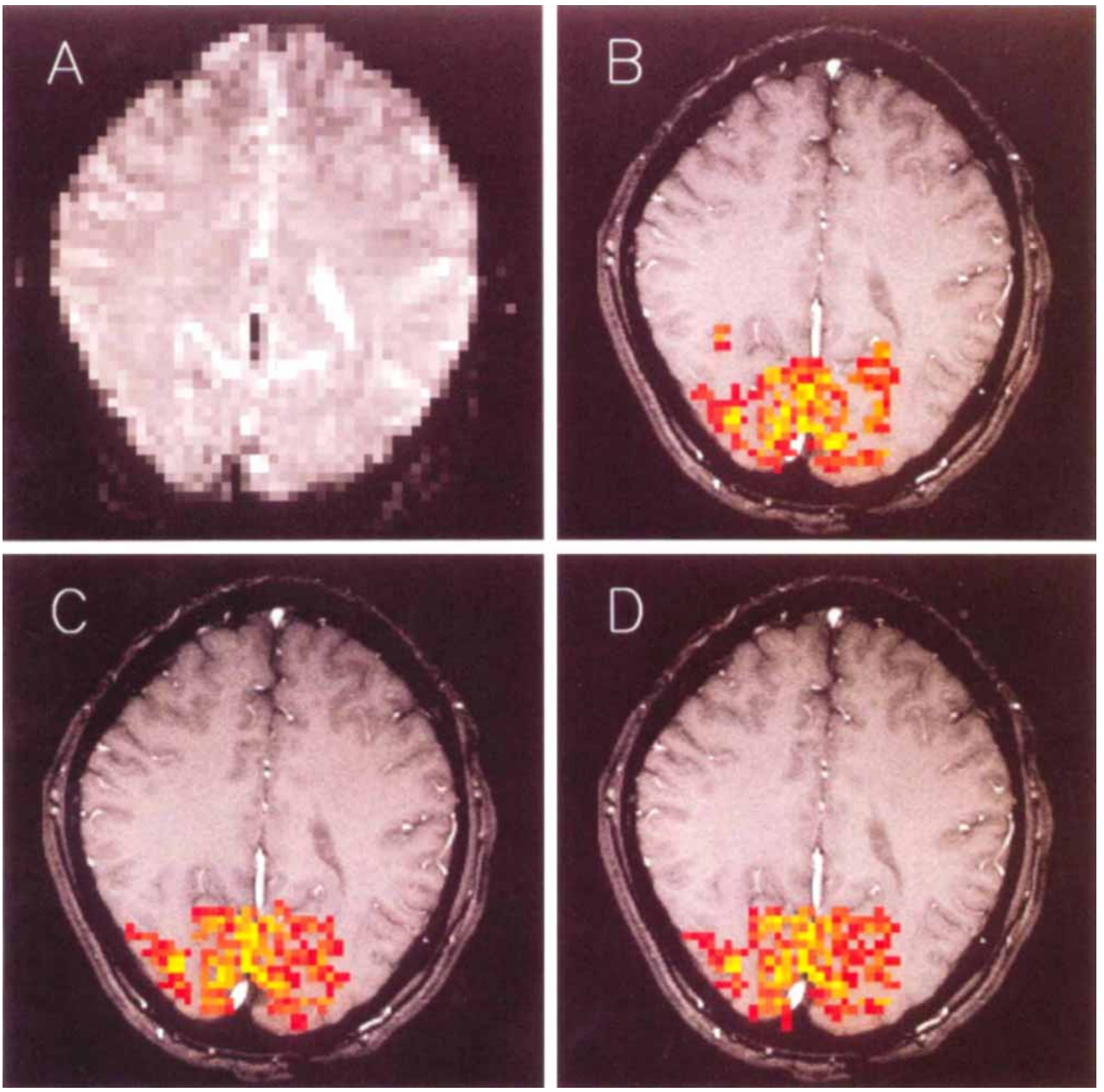

FIG. 1. (A) Spin-density-weighted image with T_2^* sensitivity (single-shot blipped gradient-echo EPI, TR = 400 ms, TE = 54 ms, flip angle = 30°, 3 × 3 × 4 mm^3 resolution) depicting the quality of oxygenation-sensitized acquisitions used for mapping functional responses to visual activation. (B–D) Color-coded activation maps superimposed onto an anatomical reference image (RF-spoiled FLASH , TR = 70 ms, TE = 6 ms, flip angle = 60°) demonstrating spatial congruence of brain regions activated by (B) a 1.6-s/8.4-s protocol, (C) a 10-s/20-s protocol, and (D) a 10-s/90-s protocol of visual activation (15 Hz, reversing black and white checkerboard versus darkness, same subject).

crease of the baseline MRI signal intensity during ongoing repetitive activation arises from the accumulation of individual signal undershoot phases already described in 1992 for slightly different experimental conditions (5). Here, the oxygenation-sensitive response reaches a new equilibrium after four to five activation cycles with the relative signal strength almost 2% below prestimulation baseline. On the other hand, the relative peak-to-peak signal difference or functional contrast, i.e., the signal strength during stimulation versus that during a control phase, remains almost unchanged throughout the experiment at approximately 4%. The end of repetitive stimulation is characterized by a slow recovery of the BOLD MRI signal decrease requiring approximately 90 s for returning to prestimulation baseline.

It is common practice to visualize details of the temporal response profile with use of time-locked averages of multiple activation cycles. It turns out that the mean response for all 12 cycles (Fig. 2B) exhibits an apparent interstimulus baseline during steady-state conditions, i.e., after the first four cycles, much lower than the true prestimulation baseline. To better link the mean re-

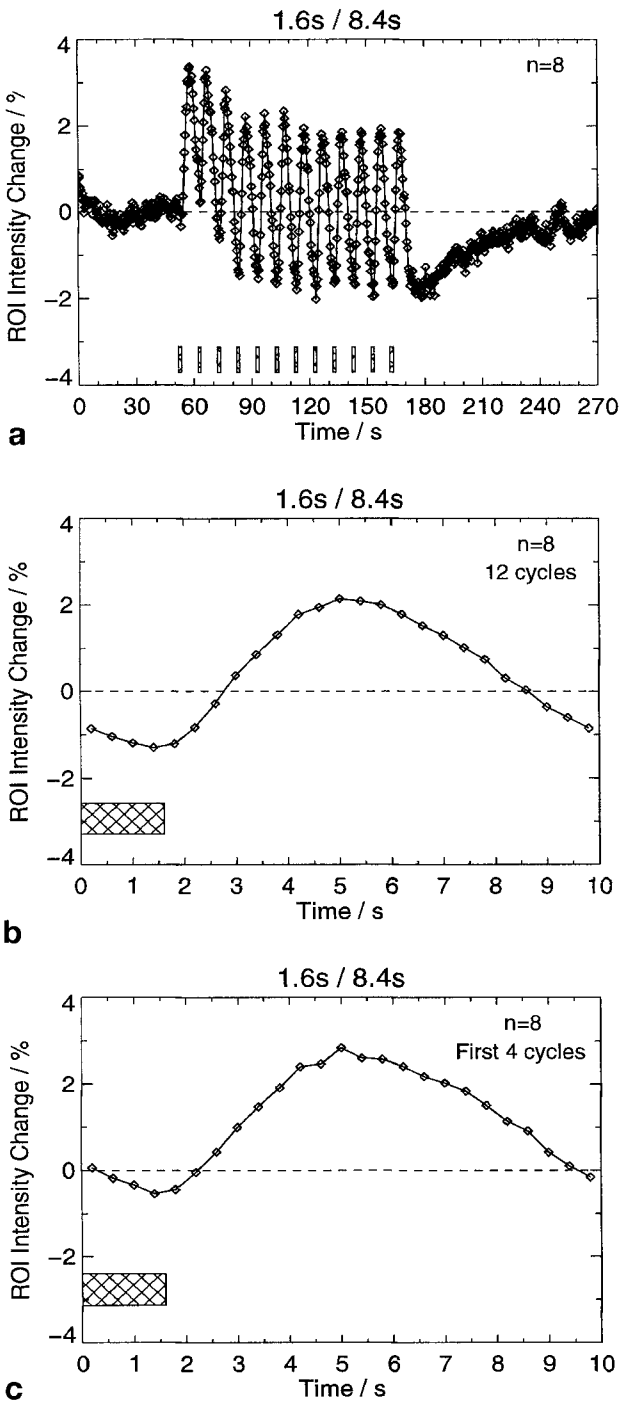

FIG. 2. Normalized time courses of BOLD MRI signal intensities (0.4-s temporal resolution) for a protocol comprising 12 cycles of 1.6 s of visual activation (cross-hatched bar) and 8.4 s of darkness. The curves represent mean values of all pixels with statistically significant stimulus-related signal alterations averaged across subjects (n = 8). (a) Real-time data set of the entire protocol, (b) time-locked average of all 12 repetitive cycles of 10-s duration, and (c) time-locked average of only the first four repetitive cycles, as in ref. 11.

sponse to the initial condition, Moore *et al.* (11) used only four cycles during the approach to steady state. Although the signal now starts and ends close to baseline values (Fig. 2C), this must be considered somewhat artificial because almost arbitrary values may be obtained by varying the number of averaged cycles. Under the chosen conditions, the resulting profile reveals a relative signal decrease of approximately 0.5% at 1.5–2.0 s after the onset of stimulation and thus qualitatively reproduces the finding of Moore *et al.* (11). In this form, it fulfills the expectation of an MRI initial dip, representing a relative deoxygenation.

The 1.6-s/90-s Protocol

In close analogy to Fig. 2, the set of mean time courses shown in Fig. 3 refers to the real-time data of a 1.6-s/90-s protocol (Fig. 3A) and time-locked averages of all four activation cycles covering either a 90-s period (Fig. 3B) or only the first 10 s in a presentation comparable to that of Fig. 2C (Fig. 3C). This protocol is identical to that of Fig. 2, except for the extension of the control period from 8.4 to 90 s. The purpose of the experiment is to ensure complete recovery of the MRI signal response to prestimulation baseline before application of a successive stimulus and thereby effectively decouple the individual responses from each other.

In agreement with the preceding protocol, the initial positive signal increase amounts to approximately 4%. In addition, the data again demonstrate that a 1.6-s stimulus provokes a marked and extended poststimulus undershoot with a maximum amplitude of −1%. These findings are in contrast to the study by Hu *et al.* (10) using control periods of 25–30 s, in which no undershoot was found for a 2.4-s stimulus but an undershoot was found for a 4.8-s stimulus. Although the exact reason for this discrepancy is difficult to assess, it may be caused by MRI contrast (e.g., residual T_1 weighting when using segmented EPI) and subtle differences in stimulus quality or presentation or may reflect the establishment of an apparent interstimulus baseline in the steady state of a repetitive protocol that nevertheless is well below the true prestimulation baseline (compare Figs. 2A and 4A).

An enlarged view of the first 10 s of the 1.6-s/90-s protocol (Fig. 3C) underlines the absence of an initial dip. The response profile is characterized by a 1.5- to 2.0-s hemodynamic latency, a positive 4% signal increase starting from prestimulation baseline and peaking at 5–7 s after stimulus onset, and an undershoot with signal intensities drifting below baseline at approximately 9 s after the end of the stimulus. Return to prestimulation baseline is accomplished 60–90 s after the end of the stimulus.

In view of these findings, the observation of an initial signal decrease for the 1.6-s/8.4-s protocol must be ascribed to a wraparound effect in the temporal profiles obtained by time-locked averaging of rapidly repeated activation cycles. Thus, an MRI signal that has not yet fully recovered at the end of an activation cycle will overlap with the response to the next stimulus and even dominate the resulting signal during the "silent" hemodynamic latency phase before the onset of the positive oxygenation-sensitive response. Instead of indicating an early deoxygenation due to a *rapid* increase of oxygen consumption, this formation of a dip reflects contribu-

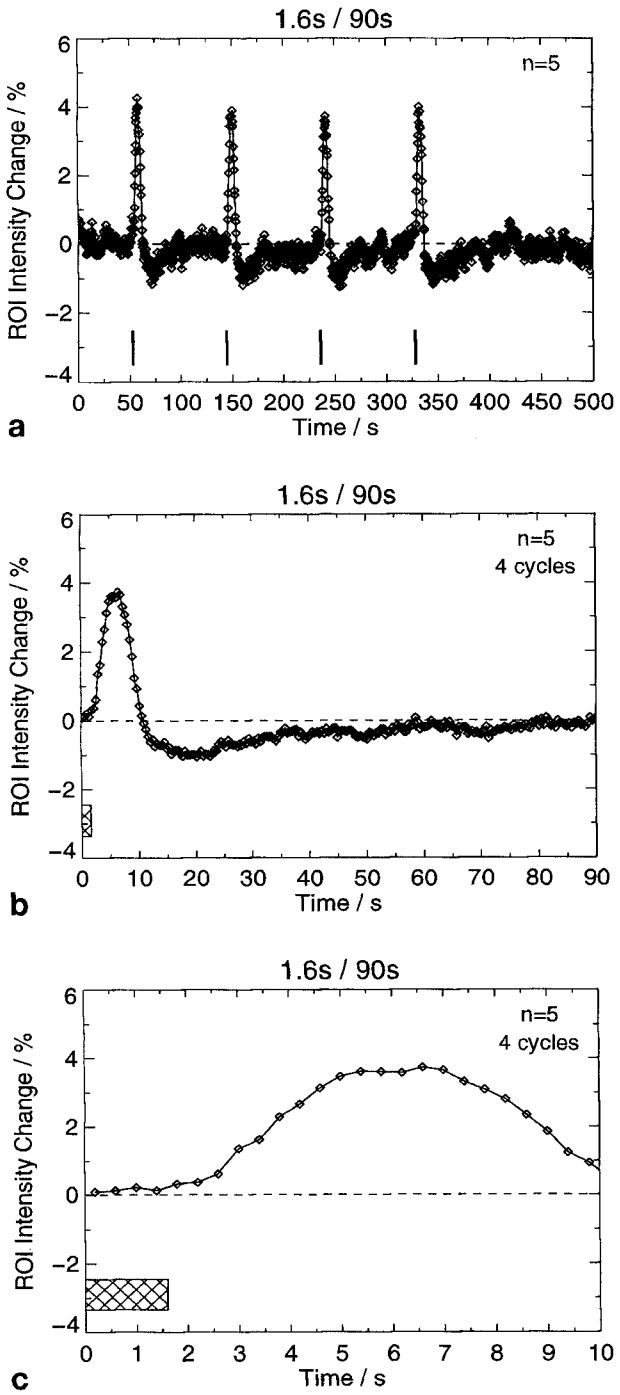

FIG. 3. Normalized time courses of BOLD MRI signal intensities (0.4-s temporal resolution) for a protocol comprising four cycles of 1.6 s of visual activation (cross-hatched bar) and 90 s of darkness. The curves represent mean values of all activated pixels averaged across subjects (n = 5). (a) Real-time data set of the entire protocol, (b) time-locked average of all four repetitive cycles of 90-s duration, and (c) time-locked average of only the first 10 s.

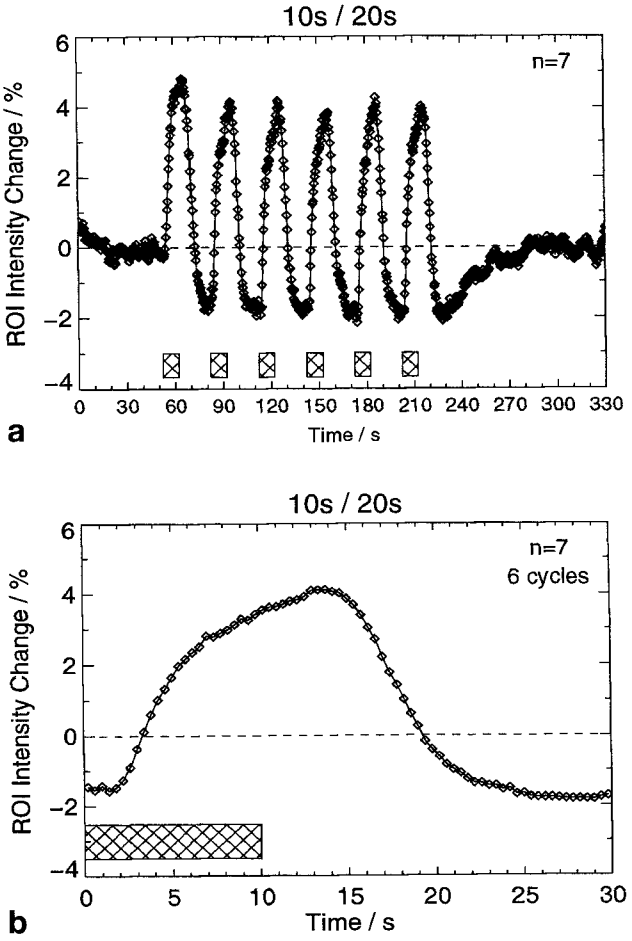

FIG. 4. Normalized time courses of BOLD MRI signal intensities (0.4-s temporal resolution) for a protocol comprising six cycles of 10 s of visual activation (cross-hatched bar) and 20 s of darkness. The curves represent mean values of all activated pixels averaged across subjects (n = 7). (a) Real-time data set of the entire protocol, (b) time-locked average of all six repetitive cycles of 30-s duration.

tions from a *slow* process of relative deoxygenation that is folded back into the early phase by the specific choices for data acquisition and analysis. Whether the evolution of a signal undershoot, its cumulative effect in the form of a baseline decrease, and its recovery indeed reflect the regulation of oxidative metabolism cannot be determined by the present study.

The 10-s/20-s Protocol

In Fig. 4, the mean time courses of a 10-s/20-s protocol are shown in real time (Fig. 4A) and as a time-locked average from all six cycles (Fig. 4B). This paradigm represents typical timings that are most frequently used for qualitative mapping of human brain function. In fact, pertinent combinations of stimulation and recovery phases, i.e., of positive signal responses and subsequent signal undershoot effects, often enhance the peak-to-peak signal differences, here to approximately 6%. In the time-locked profile, where responses are dominated by the steady-state behavior reached after two cycles, the initial signal is significantly below prestimulation baseline because of the pronounced 2% undershoot elicited by the 10-s stimulus. This observation is in agreement with corresponding findings for the 1.6-s/8.4-s protocol, which also uses an inadequately short control period

(Fig. 2B). The recovery time for the oxygenation-sensitive response after the last stimulus is approximately 80 s.

The 10-s/90-s Protocol

Analogous to the temporal profiles obtained for the first and second protocol, a full decoupling of individual responses to a repetitive protocol of 10-s visual activation may be achieved by increasing the control period to 90 s. In Fig. 5, the mean time courses are shown in real time (Fig. 5A) and as time-locked averages of four activation cycles covering either the full 100-s protocol (Fig. 5B) or only the first 10 s (Fig. 5C) comparable to Figs. 2C and 3C. Here, the peak-to-peak signal difference is almost 8% emerging from a 6% positive response and a 2% undershoot that exhibits a duration of approximately 80 s. An enlarged view at the first 10 s of the time-locked average demonstrates that the MRI signal response starts at the prestimulation baseline with no initial signal decrease.

The findings for a 10-s stimulus are in excellent agreement with those for the 1.6-s stimulus and further support the view that BOLD MRI responses to visual activation are the result of more than just one hemodynamic adjustment with one time constant. Although both the positive oxygenation-sensitive response and the undershoot phenomenon are amplified by the longer stimulus, there are no qualitative differences in the temporal response profile for a 1.6-s stimulus and a 10-s stimulus. The responses to successive stimuli become completely independent from each other when the recovery phase is extended to 90 s. Under such conditions, the MRI signal strength of each activation cycle returns to prestimulation baseline with no detectable signal decrease during the early phase.

Evidence for an Initial Dip?

Because mean responses averaged across subjects partially suppress intersubject variations and therefore may obscure the detectability of an early signal decrease, all signal time courses for the 10-s/90-s protocol were also analyzed on an individual basis. An initial dip was found in one of seven subjects, as shown in Fig. 6. The time courses represent time-locked averages of all four activation cycles for the whole protocol of 100 s (Fig. 6A) and only the first 10 s (Fig. 6B).

To allow for spatial heterogeneity with a possibility of further enhancing the initial signal decrease in this subject, Fig. 6C shows a time course of a subpopulation of activated pixels selected for maximum correlation with the reference function. It turns out that these pixels not only yield an early signal decrease of approximately 0.5% peaking at 1.5 s after the onset of stimulation but also give the strongest positive responses above the mean level (Fig. 6B) as well as a pronounced undershoot effect. Such pixels were mainly found in or around macroscopic vessels, whereas "parenchymal" signals resulted in weaker responses but no initial signal decrease in any chosen subpopulation of activated pixels. However, acquisitions at much higher spatial resolution and more sophisticated spatial analyses are needed to clarify this issue.

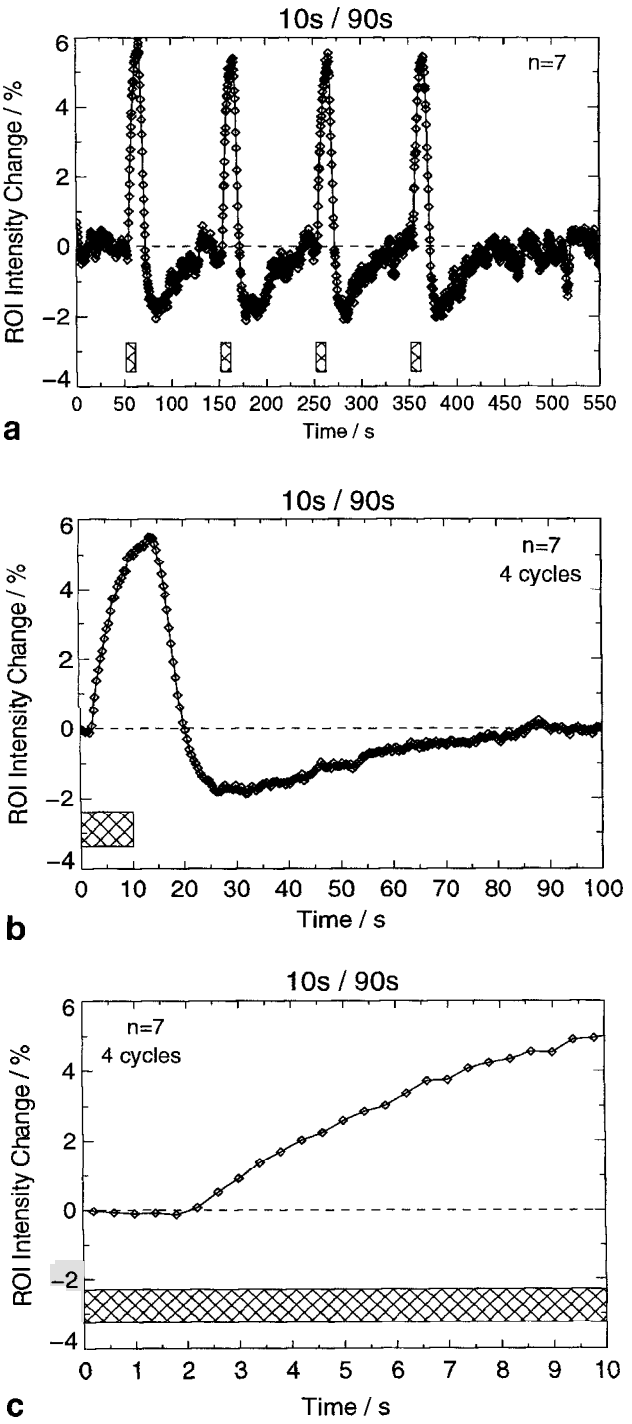

FIG. 5. Normalized time courses of BOLD MRI signal intensities (0.4-s temporal resolution) for a protocol comprising four cycles of 10 s of visual activation (cross-hatched bar) and 90 s of darkness. The curves represent mean values of all activated pixels averaged across subjects (n = 7). (a) Real-time data set of the entire protocol, (b) time-locked average of all four repetitive cycles of 100-s duration, and (c) time-locked average of only the first 10 s.

CONCLUSION

In summary, the temporal profiles of MRI-detected responses to visual activation depend on the history of preceding activations. This finding applies to most experimental conditions currently in use for mapping hu-

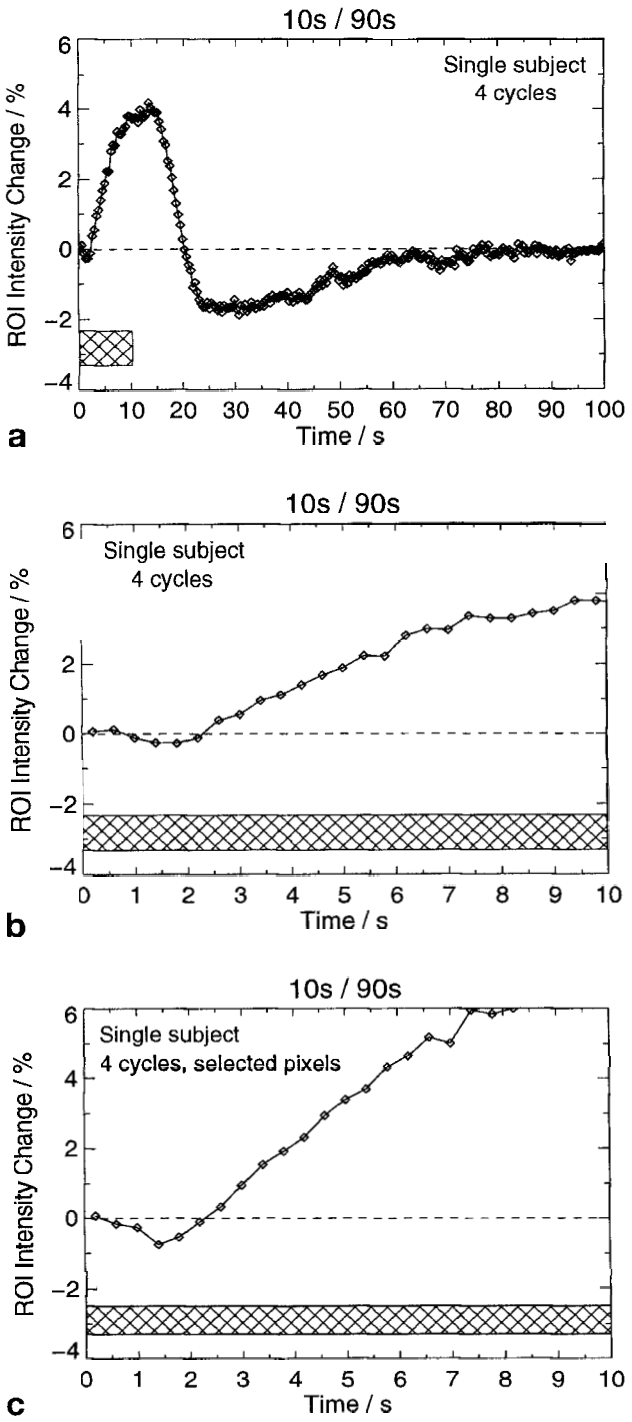

FIG 6. Normalized time courses of a single subject exhibiting an initial dip. The curves represent time-locked averages of BOLD MRI signal intensities from all four repetitive cycles (0.4-s temporal resolution) for a protocol comprising 10 s of visual activation (cross-hatched bar) and 90 s of darkness. (a) Responses from all activated pixels for the entire cycle of 100-s duration and (b) for only the first 10 s. (c) The observation of an initial dip is enhanced for a subpopulation of pixels exhibiting maximum correlation with the reference function.

man brain function. In particular, it affects the detectability of an early MRI signal change: rather than representing true upregulation of oxygen consumption during the first few seconds after stimulus onset, such a phenomenon may occur as the result of a wraparound effect when using time-locked averages of signal time courses derived from multiple activation cycles. In general, repetitive stimuli may lead to deceptive results and interpretations if the recovery period between successive stimuli is too short. The present results indicate that repetitive visual activation with a reversing black and white checkerboard for durations of 1.6–10 s requires a control state with a duration of at least 90 s to ensure complete decoupling of individual responses.

The physiological details of the hemodynamic and/or metabolic phenomena that occur in association with a change in focal neuronal activity are not yet entirely clear. For example, it is still under debate whether the processes that involve a slow response to visual activation, e.g., the poststimulus undershoot or the signal decrease reported during sustained activation, may be ascribed to adjustments in blood flow, blood volume, or oxidative metabolism. Similarly, the question of whether a fast response or initial dip may be consistently observed in signal intensity time courses of oxygenation-sensitized MR images requires further experimental support. Although the latter issue was not the primary subject of this work, the present findings indicate that any physiological investigation of functional brain activation should be based on paradigms that avoid complications from protocol timings. Conversely, a mere qualitative utilization of BOLD contrast for mapping the functional anatomy of the human brain may benefit from the temporal response characteristics to successive stimuli by maximizing the physiologically driven MRI contrast between alternating states of neuronal activity.

REFERENCES

1. S. Ogawa, T. M. Lee, A. R. Key, D. W. Tank, Brain magnetic resonance imaging with contrast dependent on blood oxygenation. *Proc. Natl. Acad. Sci. U S A* **87**, 9868–9872 (1990).
2. K. K. Kwong, J. W. Belliveau, D. A. Chesler, I. E. Goldberg, R. M. Weisskoff, B. P. Poncelet, D. N. Kennedy, B. E. Hoppel, M. S. Cohen, R. Turner, H. M. Cheng, T. J. Brady, B. R. Rosen, Dynamic magnetic resonance imaging of human brain activity during primary sensory stimulation. *Proc. Natl. Acad. Sci. U S A* **89**, 5675–5679 (1992).
3. S. Ogawa, D. W. Tank, R. Menon, J. M. Ellermann, S. G. Kim, H. Merkle, K. Ugurbil, Intrinsic signal changes accompanying sensory stimulation: functional brain mapping with magnetic resonance imaging. *Proc. Natl. Acad. Sci. U S A* **89**, 5951–5955 (1992).
4. P. A. Bandettini, E. C. Wong, R. S. Hinks, R. S. Tikofsky, J. S. Hyde, Time course EPI of human brain function during task activation. *Magn. Reson. Med.* **25**, 390–397 (1992).
5. J. Frahm, H. Bruhn, K. D. Merboldt, W. Hänicke, Dynamic MRI of human brain oxygenation during rest and photic stimulation. *J. Magn. Res. Imaging* **2**, 501–505 (1992).
6. G. Krüger, A. Kleinschmidt, J. Frahm, Dynamic MRI sensitized to cerebral blood oxygenation and flow during sustained activation of human visual cortex. *Magn. Reson. Med.* **35**, 797–800 (1996).
7. P. A. Bandettini, K. K. Kwong, T. L. Davis, R. B. H. Tootell, E. C. Wong, P. T. Fox, J. W. Belliveau, R. M. Weisskoff, B. R. Rosen, Characterization of cerebral blood oxygenation and flow changes during prolonged brain activation. *Hum. Brain Mapping* **5**, 93–109 (1997).
8. G. Krüger, A. Kleinschmidt, J. Frahm, Stimulus-dependence of cerebral blood oxygenation changes during sustained activation of human visual cortex. *Neuroimage* **5**, S36 (1997).
9. R. S. Menon, S. Ogawa, X. Hu, J. P. Strupp, P. Anderson, K. Ugurbil, BOLD based functional MRI at 4 Tesla includes a capillary bed contribution: echo-planar imaging correlates with previous optical

imaging using intrinsic signals. *Magn. Reson. Med.* **33,** 453–459 (1995).
10. X. Hu, T. H. Le, K. Ugurbil, Evaluation of the early response in fMRI in individual subjects using short stimulus duration. *Magn. Reson. Med.* **37,** 877–884 (1997).
11. G. G. Moore, Y. T. Zhang, D. B. Twieg, Assessment of the fast response spatial distribution, *in* "Proc., ISMRM, 5th Annual Meeting, Vancouver, 1997," p. 377.
12. T. Ernst, L. Chang, Early signal drop after visual stimulation observed with a gated Turbo-FLASH sequence, *in* "Proc., ISMRM, 5th Annual Meeting, Vancouver, 1997," p. 744.
13. A. Vazquez, S. Peltier, D. Davis, D. Noll, Evidence of the fast response at 3.0 T, *in* "Proc., ISMRM, 5th Annual Meeting, Vancouver, 1997," p. 726.
14. T. Ernst, J. Hennig, Observation of a fast response in functional MR. *Magn. Reson. Med.* **32,** 146–149 (1994).
15. C. Janz, J. Hennig, O. Speck, Further elucidation of the signal time course in the visual cortex following multiple short stimuli in fMRS, *in* "Proc., ISMRM, 5th Annual Meeting, Vancouver, 1997," p. 724.
16. R. D. Frostig, E. E. Lieke, D. Y. Ts'o, A. Grinwald, Cortical functional architecture and local coupling between neuronal activity and the microcirculation revealed by in vivo high-resolution optical imaging of intrinsic signals. *Proc. Natl. Acad. Sci. U S A* **87,** 6082–6086 (1990).
17. A. Grinwald, R. D. Frostig, R. M. Siegel, R. M. Bartfeld, High-resolution optical imaging of functional brain architecture in the awake monkey. *Proc. Natl. Acad. Sci. U S A* **88,** 11559–11563 (1991).
18. D. Malonek, A. Grinwald, Interactions between electrical activity and cortical microcirculation revealed by imaging spectroscopy: implications for functional brain mapping. *Science* **272,** 551–554 (1996).
19. P. A. Bandettini, A. Jesmanowicz, E. C. Wong, J. S. Hyde, Processing strategies for time-course data sets in functional MRI of the human brain. *Magn. Reson. Med.* **30,** 161–173 (1993).
20. A. Kleinschmidt, M. Requardt, K. D. Merboldt, J. Frahm, On the use of temporal correlation coefficients for magnetic resonance mapping of functional brain activation: individualized thresholds and spatial response delineation. *Intern. J. Imag. Sys. Technol.* **6,** 238–244 (1995).